

Supplementary Material

Catalytic effects of photogenerated Fe(II) on the ligand-controlled dissolution of Iron(hydr)oxides by EDTA and DFOB

Jagannath Biswakarma ^{a,b}, Kyounglim Kang ^c, Walter D.C. Schenkeveld ^d, Stephan M. Kraemer ^c,
Janet G. Hering ^{a,b,e} and Stephan J. Hug ^{b,*}

^a Swiss Federal Institute of Technology (ETH) Zurich, IBP, CH-8092 Zürich, Switzerland

^b Eawag, Swiss Federal Institute of Aquatic Science and Technology, CH-8600 Dübendorf,
Switzerland

^c University of Vienna, Dept. of Environmental Geosciences, 1090 Vienna, Austria

^d Copernicus Institute of Sustainable Development, Faculty of Geosciences, Utrecht University,
3584 CB Utrecht, the Netherlands

^e Swiss Federal Institute of Technology Lausanne (EPFL), ENAC, CH-1015 Lausanne, Switzerland

* Corresponding author. E-mail: stephan.hug@eawag.ch

Table S1	List of chemicals
Table S2	List of dissolution rates and catalytic effects compared with previous studies
Tables S3	S3a: Model input for Acuchem S3b: Rate coefficients used for the fits shown in Figures 2-4
Figure S1	Emission spectrum of the UV-source and absorbance spectra of Lp, Gt, Fe(III)EDTA and Fe(III)DFOB.
Figure S2	Speciation of Fe(II) in the presence of DFOB , EDTA and phenanthroline
Figure S3	Determination of photoproduced Fe(II)
Figure S4	Formation of Fe(III)EDTA
Figure S5	Formation of Fe(III)DFOB
Figure S6	Reproducibility of Experiments
Figure S7	Infrared spectra and kinetics of EDTA and phenanthroline adsorption onto Lp
Figure S8	Comparison of EDTA vs DFOB in Lp dissolution (anoxic; pH 7.0).
Figure S9	Effect of intermittent illumination (oxic; pH 7.0): Lp dissolution with EDTA vs. DFOB
Figure S10	Comparison of Lp and Gt dissolution with 50 μ M EDTA at pH 7; anoxic conditions.
Figure S11	Infrared spectra of Lp before and after continuous illumination with UV light in aerated suspensions of Lp and EDTA/DFOB (pH 7.0)
Figure 12	Concentrations of Fe(II) and H ₂ O ₂ calculated with the kinetic model

Table S1. List of chemicals used for the current study

Chemical Name	Chemical formale	Supplier	Purity	Stock solution (mM)
Sodium Chloride	NaCl	Merck	>99%	10
Iron(II) Chloride	FeCl ₂ . 4H ₂ O	Sigma-Aldrich	>99%	10
Iron(III) Chloride	FeCl ₃ . 6H ₂ O	Sigma-Aldrich	>98%	10
EDTA (Ethylenediamine tetra acetic disodium dihydrate)	C ₁₀ H ₁₄ N ₂ Na ₂ O ₈ . 2H ₂ O	Merck	>99%	100
Mesylate salt of Desferrioxamine B	C ₂₅ H ₄₈ N ₆ O ₈ .CH ₄ O ₃ S	Sigma-Aldrich	>92.5%	100
MES (2-morpholino-ethane sulfonic acid monohydrate)	C ₆ H ₁₃ NO ₄ S.H ₂ O	Fluka	>99%	100
PIPES (Piperazine-1,4-bis(2-ethane sulfonic acid))	C ₈ H ₁₈ N ₂ O ₆ S ₂	Sigma-Aldrich	>99%	100
Sodium (bi)carbonate	NaHCO ₃	Sigma-Aldrich	>99%	3
o-Phenanthroline	C ₁₂ H ₈ N ₂ .H ₂ O	Fluka	>99%	10

Table S2. List of reported dissolution rates and catalytic effects.

Experimental conditions	Added [Fe(II)]	Lp dissolution rates			Catalytic Effect
	μM	% h ⁻¹	nM min ⁻¹	nmol s ⁻¹ m ⁻²	
(Biswakarma et al., 2020)					
20 μM DFOB, pH 7.0	0	0.08	15.2	0.04	1
(carbonate buffer)	1	0.55	103	0.27	7
	2	1.03	194	0.51	13
	5	2.14	40	1.06	26
(Kang et al., 2019)					
20 μM DFOB, pH 7.0	0	-	-	0.07	1
(MOPS)	2	-	-	0.29	4
(Biswakarma et al., 2020)					
50 μM DFOB, pH 7.0	0	0.11	20.2	0.05	1
(carbonate buffer)	1	1.44	270	0.71	13
	2	2.81	527	1.40	26
	5	6.42	1204	3.18	60
50 μM DFOB, pH 7.0	0	0.06	12	0.03	1
(MOPS buffer)	2	0.65	122	0.32	10
50 μM DFOB, pH 8.5	0	0.15	28.4	0.08	1
(PIPES buffer)	2	0.30	56.3	0.15	2
(Biswakarma et al., 2019)					
50 μM EDTA, pH 6.0	0.0	0.16		0.08	1
(MES buffer)	0.2	1.07		0.53	7
	0.5	2.29		1.14	14
	1.0	3.08		1.53	19
	2.0	3.56		1.77	22
	4.0	4.13		2.05	26
	6.0	4.17		2.07	26
	10.0	4.97		2.48	31

^{1,2} Rates measured by formation of dissolved Fe in suspensions.

³ Rates measured by decrease of FeOOH infrared bands in ATR-FTIR experiments.

Table S3a. Kinetic model as entered in Acuchem (Braun et al., 1988). ^(a)

```

; Fell catalyzed dissolution of lepidocrocite
;
input
0010
;
; Non-catalyzed dissolution
R1a, (SFe3) + L = (SFe3)L, 3.0e6 ; Adsorption of ligand
R1a, (SFe3)L = (SFe3)+L, 1.0e1 ; Desorption of ligand, K= 3e5
R1b, (SFe3)L = ( ) + Fe3L, 3.5e-5 ; Slow detachment and formation of new site
R1c, ( )+bulk = (SFe3), 1e8 ; Reformation of surface site
;
; Photochemical formation of Fe(II) and oxidants
R2ab, bulk = (SFe2)+(SFe4), 2.7E-6 ;
;R2c, (SFe2)+(SFe4) = bulk, 1e-18 ;
R2d, (SFe4)=SOHr, 1e6 ;
R2e, SOHr+SOHr = H2O2, 8.7e3 ;
;R2f, (SFe4)+L = (SFe3)+Lr, - ;
;R2g, (SFe3)L=(SFe2)+Lr, - ;
R2h, (SFe2)+bulk=(SFe3)Fe2, 1e8 ; Re-formation of surface site
;
; Adsorption/desorption of Fe2
R3, (SFe3) + Fe2 = (SFe3)Fe2, 7.2e3 ; Adsorption of Fe2
R3, (SFe3)Fe2 = (SFe3) + Fe2, 1e-3 ; Desorption of Fe2, K=7.2e6
;
; Fe(II)-catalyzed dissolution
R4a, (SFe3)Fe2 + L = (SFe2) + Fe3L, 61 ; Adsorption, ET and formation of Fe3L
R4b, (SFe3) + Fe2L = (SFe2) + Fe3L, 1.4e2 ;
R4c, (SFe3)L+Fe2 = (SFe2) + Fe3L, 2.2e4 ;
R4d, (SFe2) + bulk = (SFe3)Fe2, 1e8 ; Re-formation of adsorbed Fe2 on surface or (>1e5)
;
; Formation of dissolved Fe(II) complexes
R5, Fe2 + L = Fe2L, 5.3e9 ; Diss Fe2L formation
R5, Fe2L = Fe2 + L, 1e5 ; K=5.3e4 (DFOB)
;
; Oxidation of surface Fe(II) by dissolved O2
R6a, (SFe3)Fe2 + H2O2 = bulk + SOHr, ? ;
R6b, (SFe3)Fe2 = bulk + O2m, ? ; Oxidation of surface Fe(II) with oxygen
;
; Photolysis of dissolved Fe3L
R7a, Fe3L = Fe2 + Lr, 1e-9 ; Photolysis of Fe3L (1e-9 for DFOB)
R7b, Fe2 = Fe(OH)3, 1e-3 ;
R7c, Lr = P+ O2m, ? ;
R7d, O2m + O2m = H2O2, 1e7 ;
R7e, L + OHr = Lr, 1e9 ;
R7f, H2O2+Fe2 = OHr+Fe(OH)3, 1e3 ;
;
; Formation and reaction of oxidants in the presence of O2
R8a, (SFe2)+OHr = (Fe3), ? ;
R8b, L + SOHr = Lr, ? ;
;
End
; Starting concentrations
bulk, 1.12e-3
(SFe3), 8.5e-6
(SFe2), 0
L, 50e-6
(SFe3)Fe2, 0
(SFe3)L, 0
Fe2L, 0
Fe3L, 0
Fe2, 0
H2O2, 0
end
0.0001
? ; last time point (of 50 points ) in the model (s)
End

```

^(a) This Table corresponds to Table 2a in the main manuscript. Special characters are replaced by characters that are accepted as input for Acuchem program, for example surface species, such as $\equiv\text{Fe}^{\text{III}}\text{-O-Fe}^{\text{II}}$ were entered as (SFe3)Fe2. Equilibrium reactions, such as in reaction R1a, are expressed as forward and back reactions, with $K=k_f/k_b$ (where k_f and k_b are the rate coefficients for the forward and for the back reactions. Lines and comments starting after a semicolon are ignored by the program. This example input file is for the DFOB under anoxic condition (Fig. 3). The rate coefficients for DFOB and EDTA under the other conditions are listed in Table S3b.

Table S3b. Rate coefficients used for the fits shown in Figures 2-4. ^(a)

	Fig. 2	Fig. 2	Fig. 3	Fig. 3	Fig. 4	Fig. 4
	EDTA a	EDTA o	DFOB a	DFOB o	EDTA	DFOB
R1a,	1.0e6	1.0e6	3.0e6	3.0e6	1.0e6	3.0e6
R1a,	1.0e1	1.0e1	1.0e1	1.0e1	1.0e1	1.0e1
R1b,	3.5e-5	3.5e-5	3.5e-5	3.5e-5	3.5e-5	3.5e-5
R1c,	1e8	1e8	1e8	1e8	1e8	1e8
;						
R2ab	6.5e-6	6.5e-6	2.7E-6	2.7E-6	6.5e-6	2.7E-6
;R2c,	-	-	-	-		
R2d,	1e6	1e6	1e6	1e6	1e6	1e6
R2e,	1.6e3	1.6e3	8.7e3	8.7e3	1.4	2.4e-1
; R2f,	-	-	-	-		
;R2g,	-	-	-	-		
R2h,	1e8	1e8	1e8	1e8	1e8	1e8
R3,	7.2e3	7.2e3	7.2e3	7.2e3	7.2e3	7.2e3
R3,	1e-3	1e-3	1e-3	1e-3	1e-3	1e-3
R4a,	95	95	61	61	95	61
R4b,	6e2	6e2	1.4e2	1.4e2	1.4e2	1.4e2
R4c,	-	-	2.2e4	2.2e4	-	-
R4d,	1e8	1e8	1e8	1e8	1e8	1e8
R5,	6.0e11	6.0e11	5.3e9	5.3e9	6.0e11	5.3e9
R5,	1	1	1e5	1e5	1	1e5
R6a,	4.3e2	4.3e2	2.1E+03	2.1E+03	1.0e3	2.1e3
R6b,	1.0e-10	6.4e-3	1.1E-10	1.1E-03	5.0e-3	2.8e-3
R7a,	1.2e-4	1.2e-4	1e-9	1e-9	1.2e-4	1e-9
R7b,	1e-3	1e-3	1e-3	1e-3	1e-3	1e-3
R7c,	1e5	1e5	1e5	1e5	1e5	1e5
R7d,	1e7	1e7	1e7	1e7	1e7	1e7
R7e,	1e9	1e9	1e9	1e9	1e9	1e9
R7f,	1e3	1e3	1e3	1e3	1e2	1e3
R8a,	1e1	1e1	1e1	1e1	1e1	2.5e1
R8b,	1e1	1e1	1e1	1e1	5.0e1	1.5
Initial concentrations						
bulk	1.13e-3	1.13e-3	1.13e-3	1.13e-3	1.13e-3	1.13e-3
(SFe3)	8.5e-6	8.5e-6	8.5e-6	8.5e-6	8.5e-6	8.5e-6
(SFe2)	0	0	0	0	0	0
L	50e-6	50e-6	50e-6	50e-6	50e-6	50e-6
(SFe3)Fe2	0	0	0	0	0	0
(SFe3)L	0	0	0	0	0	0
Fe2L	0	0	0	0	0	0
Fe3L	0	0	0	0	0	0
Fe2	0	0	0	0	0	0
H2O2	0	0	0	0	0	0

^(a) For the photo-induced reactions R2ab and R7a, low values (1e-18) were entered for the dark periods. The equilibrium constants for the formation of dissolved complexes of Fe(II) with EDTA and DFOB are conditional complexation constants for pH 7.0 and 3mM NaHCO₃ calculated with Visual MINTEQ ver. 3.1 (<https://vminteq.lwr.kth.se/>).

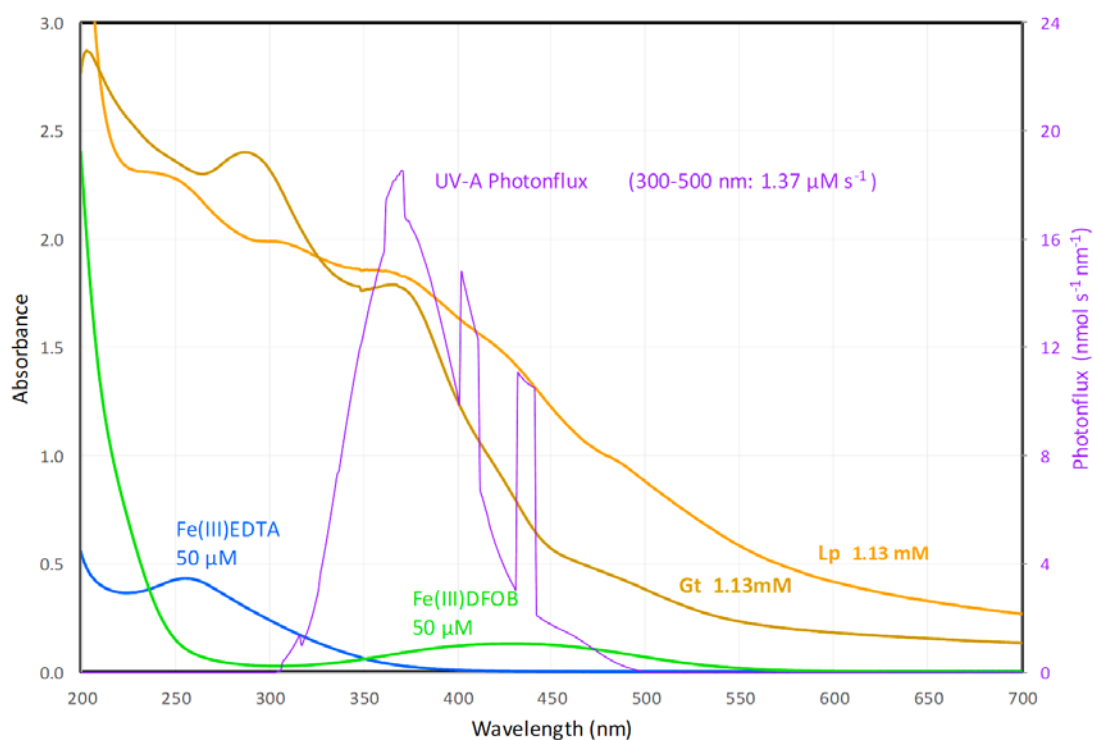


Figure S1. Emission spectrum of the UV-source and absorbance spectra of 1.13 mM Lp, 1.13 mM Gt, 50 μ M Fe(III)EDTA and 50 μ M Fe(III)DFOB. The integrated light flux from 300-500 nm was 1.37 μ mol photons s⁻¹ and was >98% absorbed by the suspensions (100 ml) in pyrex bottles of 4 cm diameter, resulting in a rate of light absorption of 13.7 Ms⁻¹ (822'000 nMs⁻¹ in Table 2a).

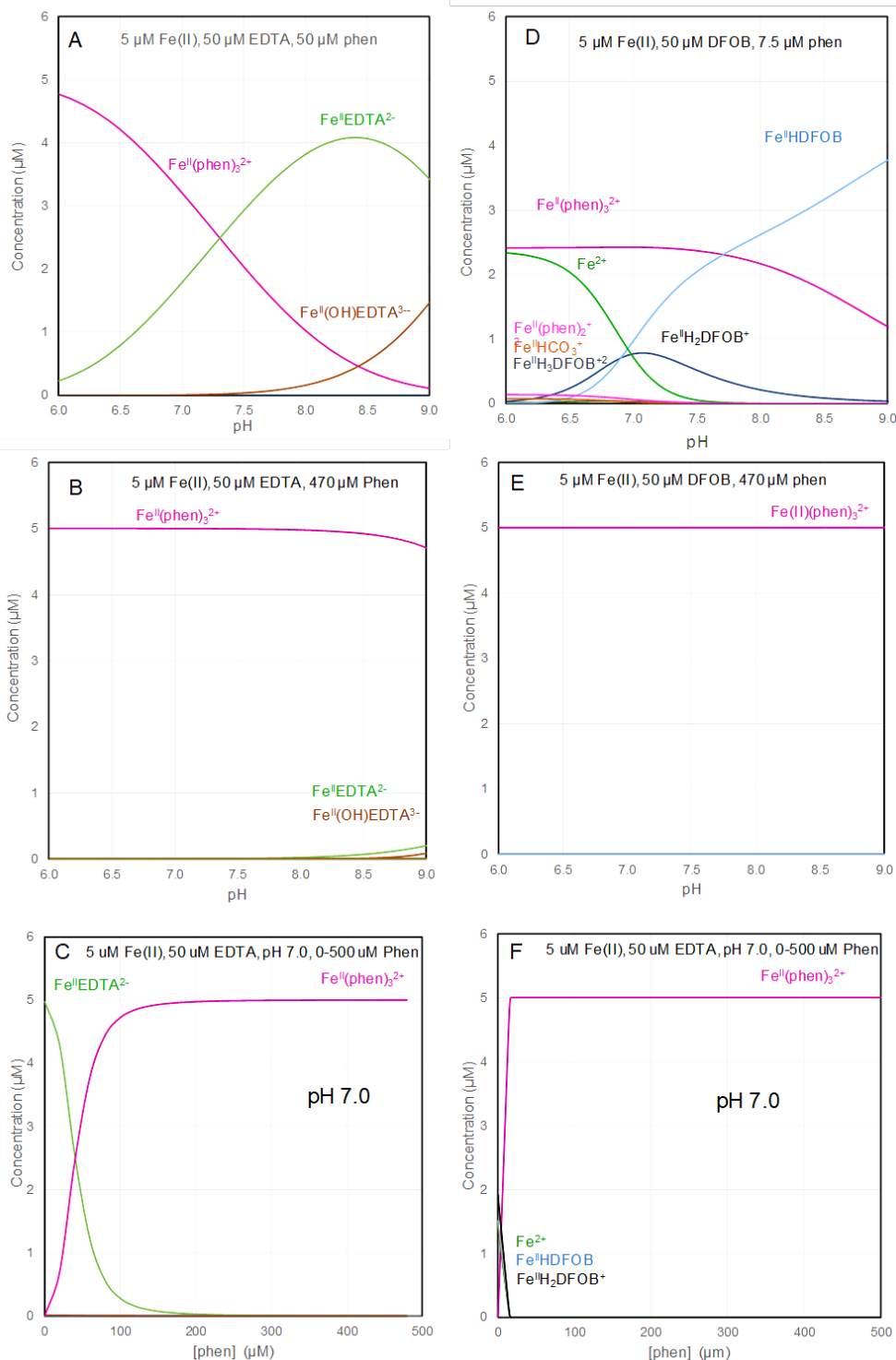


Figure S2. Speciation of Fe(II) in the presence 50 μM EDTA (A-C) or 50 μM DFOB (D-F) and 0-473 μM phenanthroline, calculated with Visual MINTEQ ver. 3.1 (<https://vminteq.lwr.kth.se/>). Concentrations of phenanthroline (phen) and pH were varied as indicated in the figures. In panels A and D, concentrations of phen were chosen low to show the pH-dependence of all relevant complexes. Panels B and E show that the applied concentration of 470 μM phen in the experiments was sufficient to complex over 99.9% of Fe(II) as $\text{Fe}^{\text{II}}(\text{phen})_3^{2+}$ at pH 7.0. Panels C and F show the concentrations of $\text{Fe}^{\text{II}}(\text{phen})_3^{2+}$ as function of the total concentration of phen at pH 7.0. Background electrolyte was 3 mM Na^+ and 3 mM Alkalinity (H_2CO_3 , HCO_3^- , CO_3^{2-}).

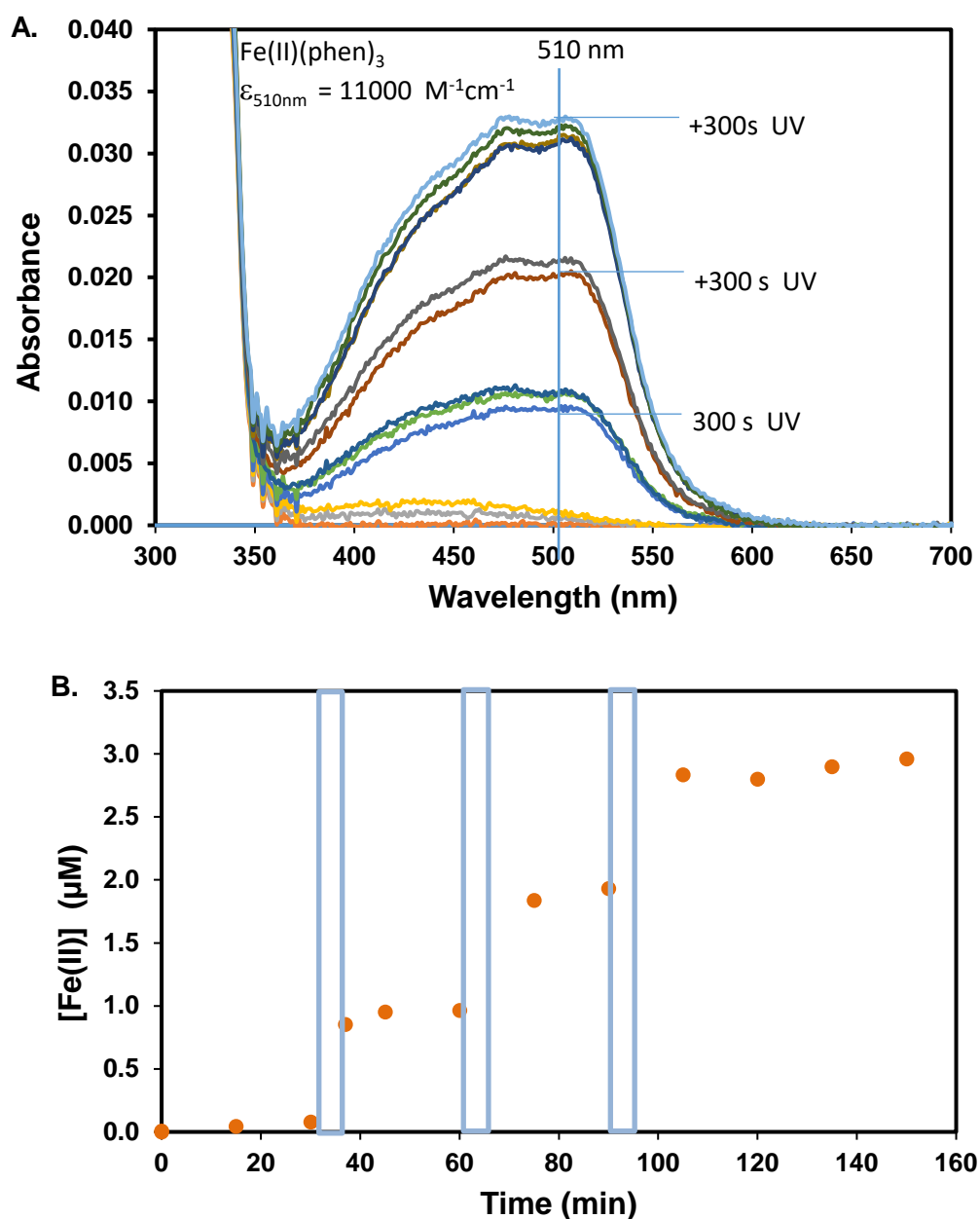


Figure S3. Determination of the photo-produced Fe(II) in a suspension of 10 mg Lp/100 ml (1125 μM Lp) with 50 μM DFOB and 473 μM phenanthroline at pH 7 (3 mM NaHCO_3 , 2% CO_2 in N_2). 2.0 ml aliquots were withdrawn and filtered (0.1 μm nylon filter) and spectra were measured in 1 cm quartz-cuvettes. Spectra (baseline corrected) are shown in Fig. S1A (top), corresponding Fe(II)-concentrations (calculated from the absorbance at 510 nm) are shown in Fig. S1B (bottom). Each 5 min illumination produced $1.0 \pm 0.1 \mu\text{M}$ Fe(II). Illumination periods (300 s) in Fig. S1B (bottom) are indicated with empty blue bars. The detection limit was 0.0005 absorbance units at 510 nm (mean of 11 data points from 505-515 nm) corresponding to 0.05 μM $\text{Fe}^{\text{II}}(\text{phen})_3^{2+}$ with $\epsilon_{510\text{ nm}} = 11000 \text{ M}^{-1}\text{cm}^{-1}$

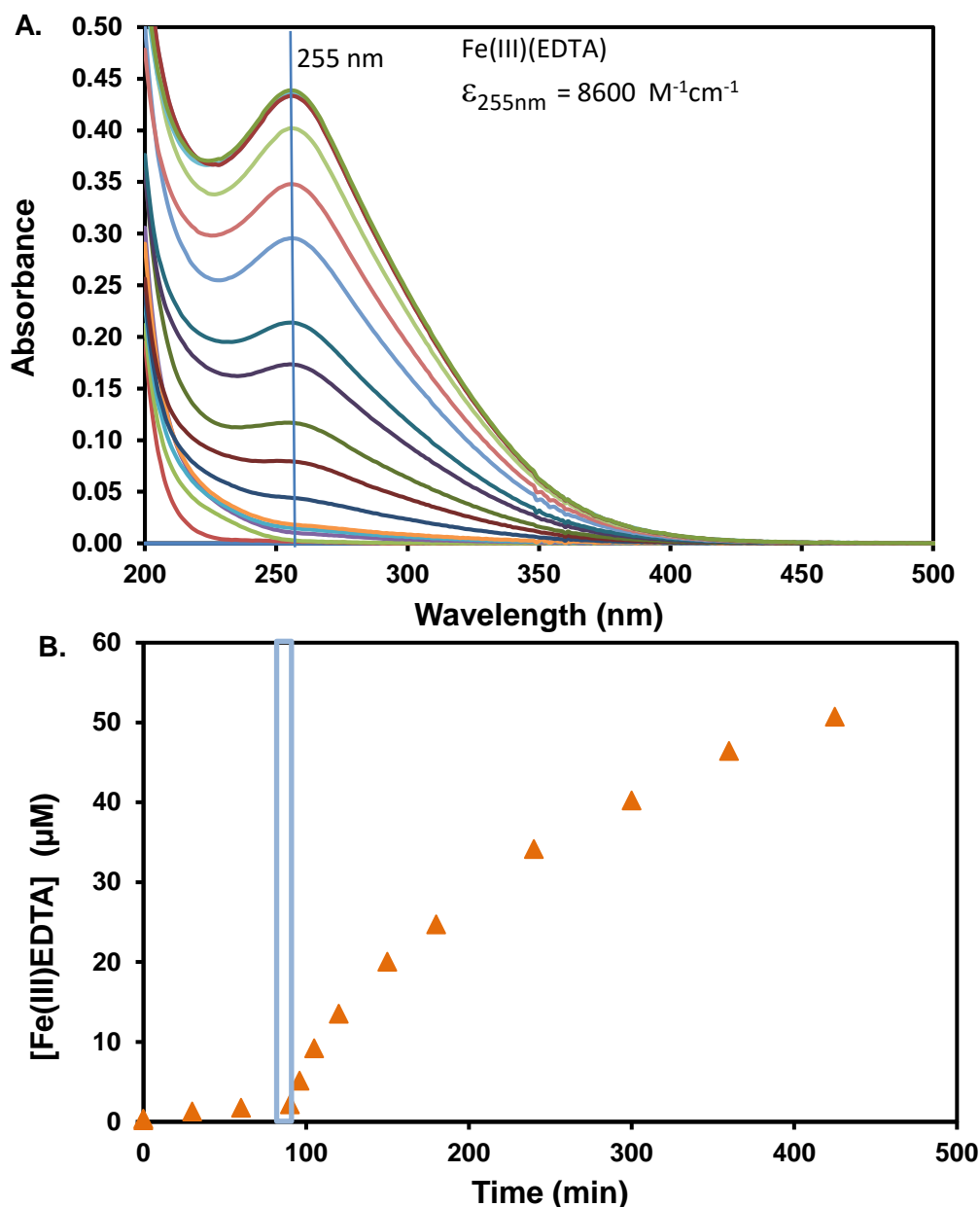


Figure S4. Formation of Fe(III)EDTA in a suspension of 10 mg/100 ml (1125 μM Lp) with 50 μM EDTA at pH 7 (3 mM NaHCO_3 , 2% CO_2 in N_2). 2.0 ml aliquots were withdrawn and filtered (0.1 μm nylon filter) and spectra were measured in 1 cm quartz-cuvettes. Spectra (baseline corrected) are shown in Fig. S2A (top), corresponding Fe(III)(EDTA)-concentrations (calculated from the absorbance at 255 nm) are shown in Fig. S2 B (bottom). UV-Illumination periods (90-95 min) is indicated with blue rectangles. The detection limit was 0.002 absorbance units at 255 nm (mean of 11 data points from 250-260 nm) corresponding to 0.23 μM Fe(III)(EDTA) with $\epsilon_{255 \text{ nm}} = 8600 \text{ M}^{-1}\text{cm}^{-1}$.

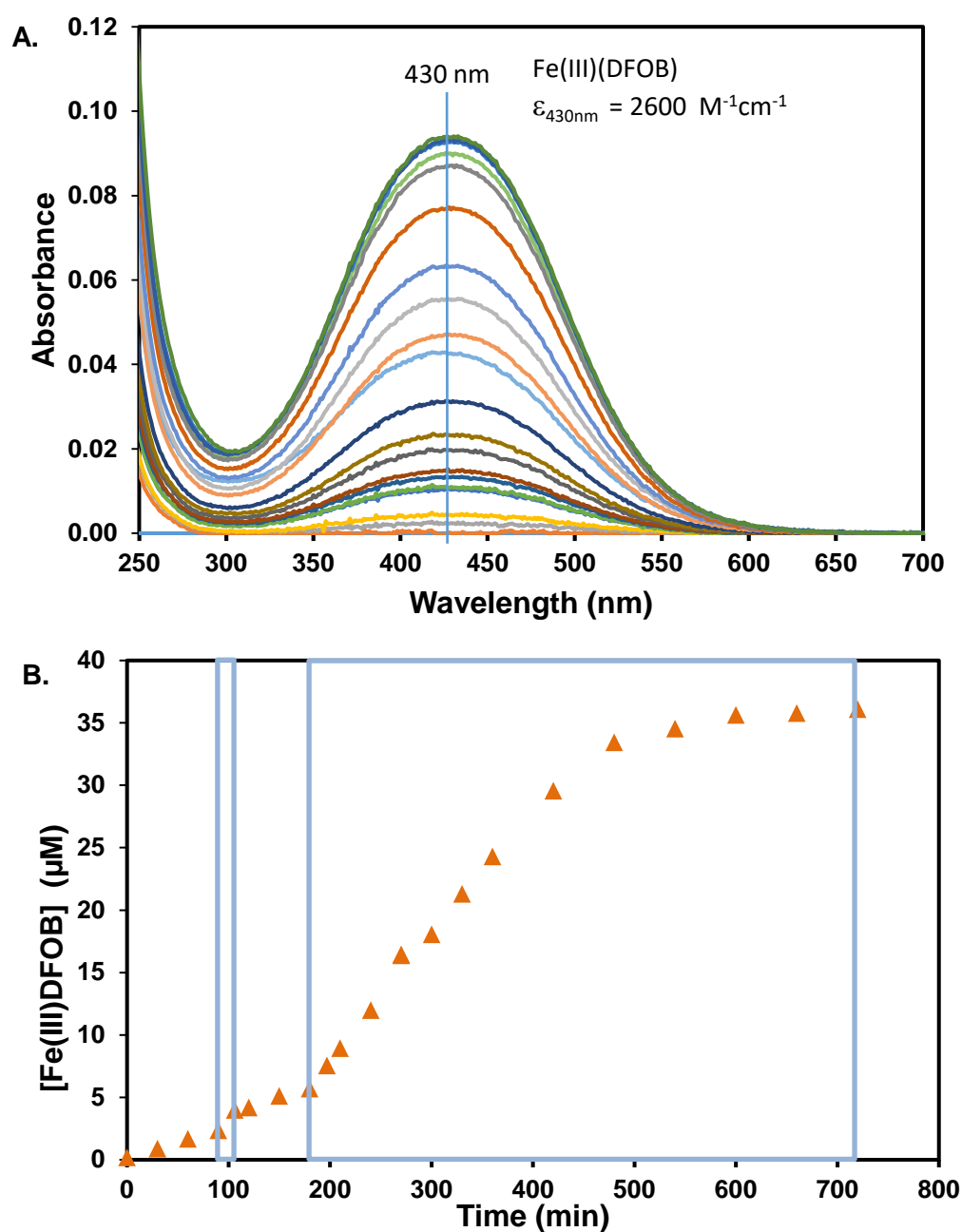


Figure S5. Formation of Fe(III)DFOB in a suspension of 10 mg/100 ml (1125 μM Lp) with 50 μM DFOB at pH 7 (3 mM NaHCO_3 , 2% CO_2 in air). 2.0 ml aliquots were withdrawn and filtered (0.1 μm nylon filter) and spectra were measured in 1 cm quartz-cuvettes. Spectra (baseline corrected) are shown in Figure A (top), corresponding Fe(III)(DFOB)-concentrations (calculated from the absorbance at 430 nm) are shown in Figure B (bottom). UV-Illumination periods (90-105 min and 180-720 min) are indicated with blue rectangles. The detection limit was 0.001 absorbance units at 430 nm (mean of 11 data points from 425-435 nm) corresponding to 0.38 μM Fe(III)DFOB complexes with $\epsilon_{430\text{ nm}} = 2600 \text{ M}^{-1}\text{cm}^{-1}$.

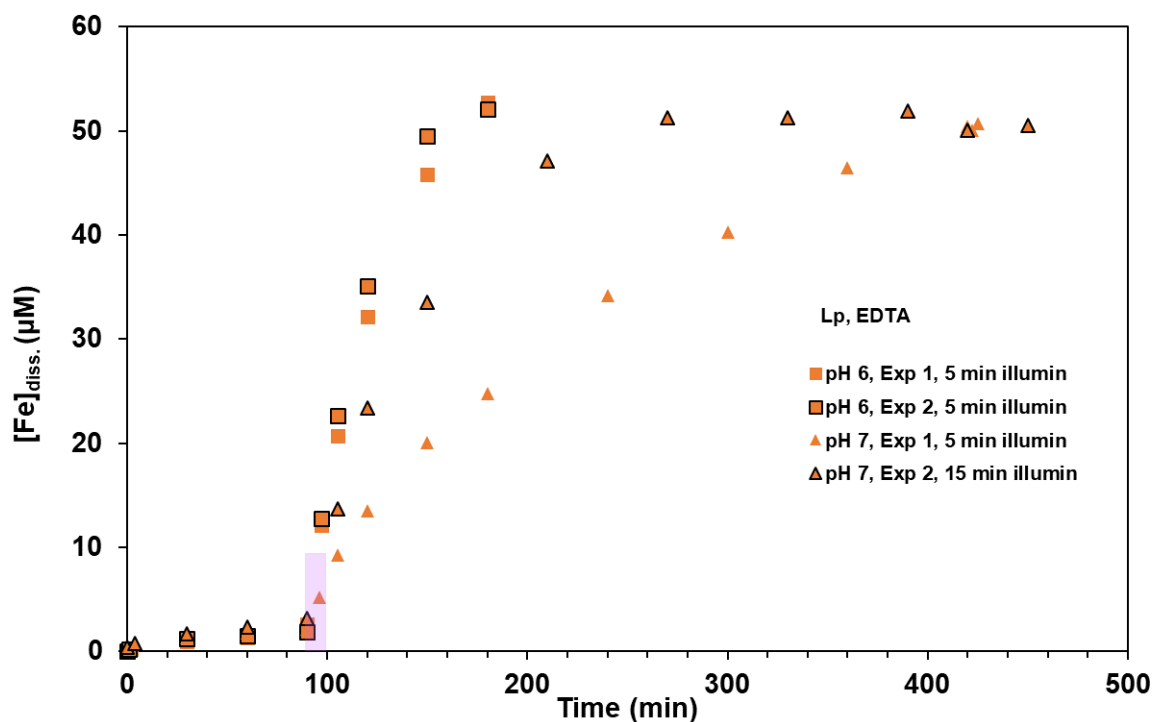


Figure S6a. Duplicate measurements; Lp dissolution in the presence of 50 μM EDTA. UV-A intermittent illumination of 5 min (shown by purple bar, 90-95 min) applied to Lp (1125 μM) suspension at pH 6 (duplicate experiments; Exp 1 and Exp. 2) and pH 7 (Exp. 1) under anoxic conditions. A 15 min illumination was applied in 90-105 min at pH 7 (Exp. 2).

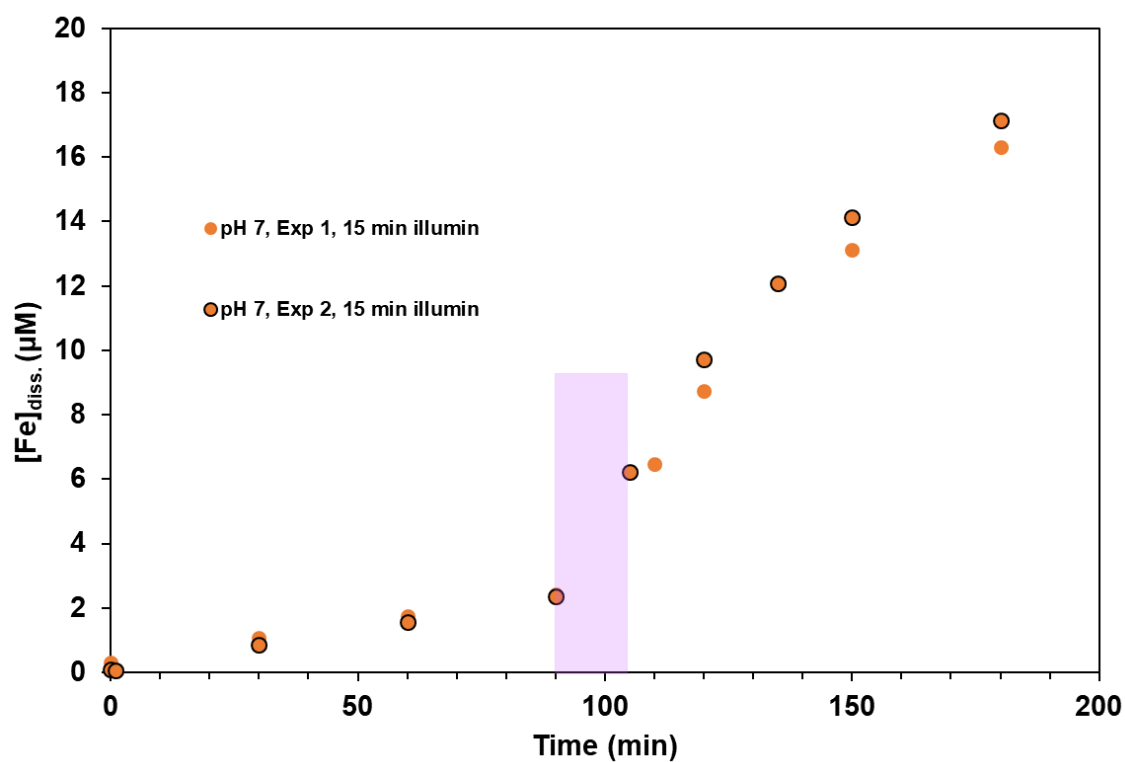


Figure S6b. Duplicate measurements; Lp dissolution in the presence of 50 μM DFOB. UV-A intermittent illumination of 15 min (shown by purple bar, 90-105 min) applied to Lp (1125 μM) suspension at pH 7.

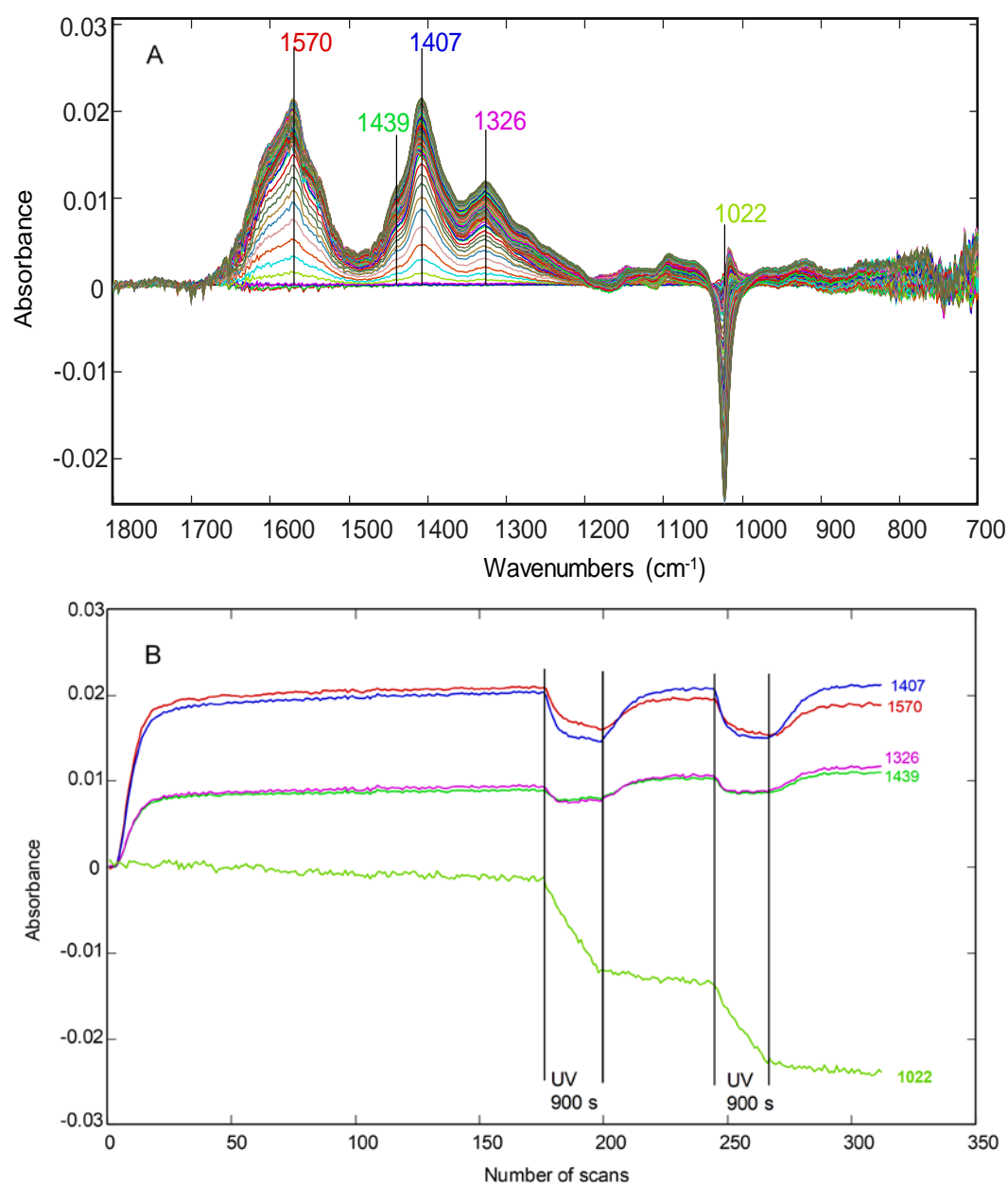


Figure S7. A. ATR-FTIR spectra collected during adsorption of EDTA (50 μM) to Lp at pH 6.0; B. the amplitudes of the peak maxima as a function of number of scans (each scan of 43 s). Phen was added between 100 and 150 min to concentration of 500 μM . No changes in the spectra of EDTA and no additional peaks due phen were observed. (Phen has absorption peaks at 1616, 1587, 1502, 1447 and 1416 cm^{-1}). (Jones et al., 2014) The peak at 1502 cm^{-1} should be observable if phen would adsorb to the surface and the other peaks would add to and increase the amplitudes shown for EDTA at 1570, 1407 and 1326 cm^{-1} . Two illuminations at 180-195 min and 245-260 min lead to a decrease of adsorption peaks of EDTA due to photodecomposition of the ligand and to a decrease of the characteristic absorbance of Lp at 1022 cm^{-1} , as described in Biswakarma et al. 2019. (Biswakarma et al., 2019) After the end of each illumination, EDTA on the surface is replenished by EDTA from solution.

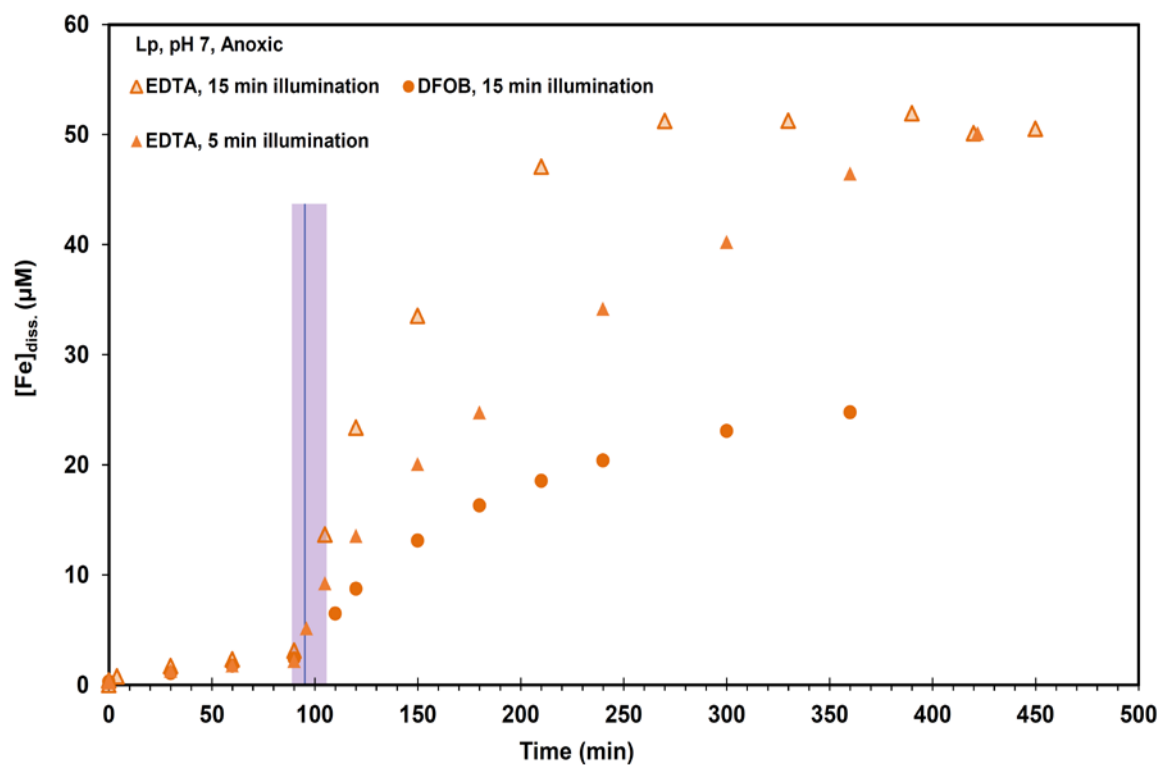


Figure S8. Comparison of EDTA vs DFOB in Lp dissolution (anoxic; pH 7.0). UV-A illuminations from 90-105 min for EDTA and DFOB, and 90-95 min for EDTA indicated with purple bar, were applied to 1.13 mM Lp suspensions in the presence of 50 μM DFOB or EDTA. Note that data for EDTA with 5 min illumination was already shown in Figure 2.

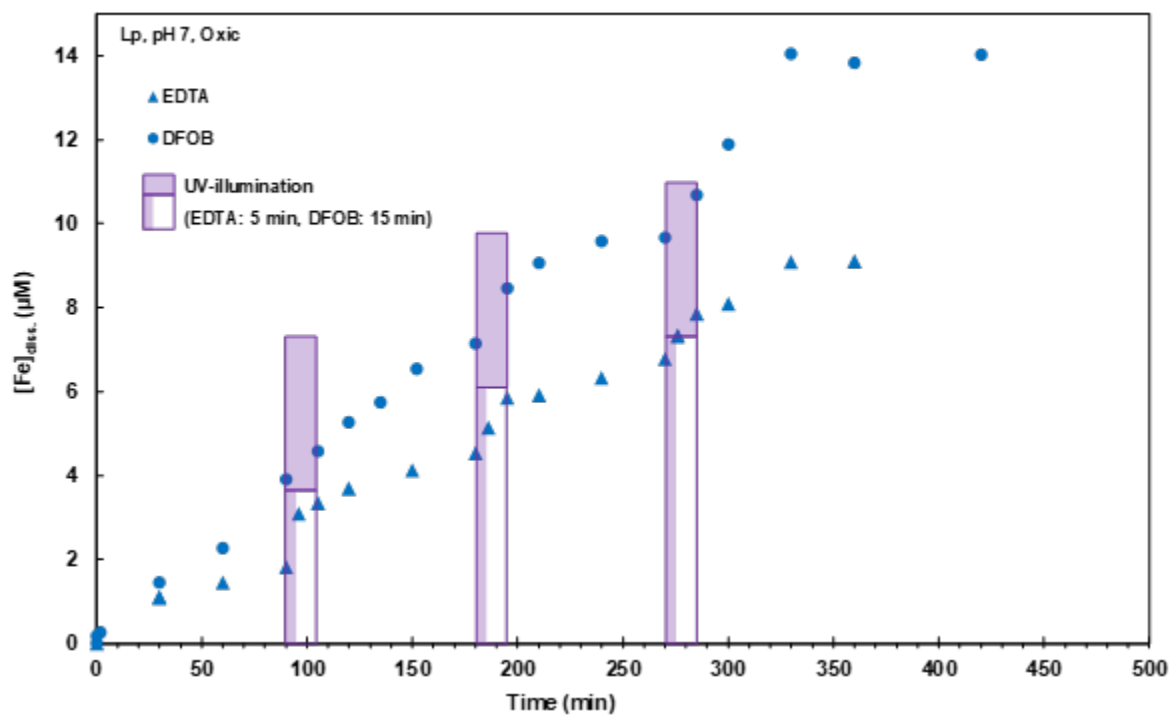


Figure S9. Comparison of EDTA vs DFOB in Lp dissolution (oxic; pH 7.0). Three intermittent illuminations (15 min for DFOB and 5 min for EDTA) were applied to 1.13 mM Lp suspension. $[\text{Fe}]_{\text{diss.}}$ was minimally increased after each illumination.

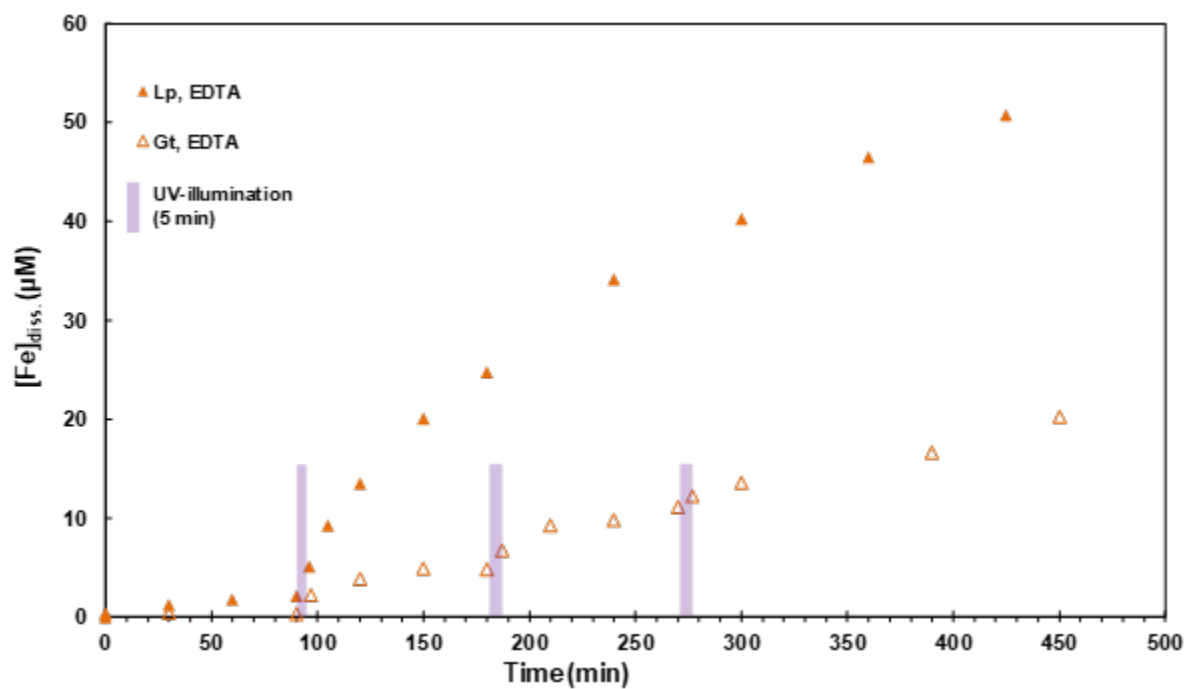


Figure S10. Comparison of Lp and Gt dissolution in the presence of 50 μM EDTA at pH 7 under anoxic conditions. The data are already shown for Lp in Fig.2 and for Gt in in Fig. 5. After one 5 min of UV illumination, accelerated Lp dissolution continued until all free EDTA in solution was used up. In contrast, three 5 min intermittent UV illuminations led to only 20 μM $[\text{Fe}]_{\text{diss}}$ in Gt suspension.

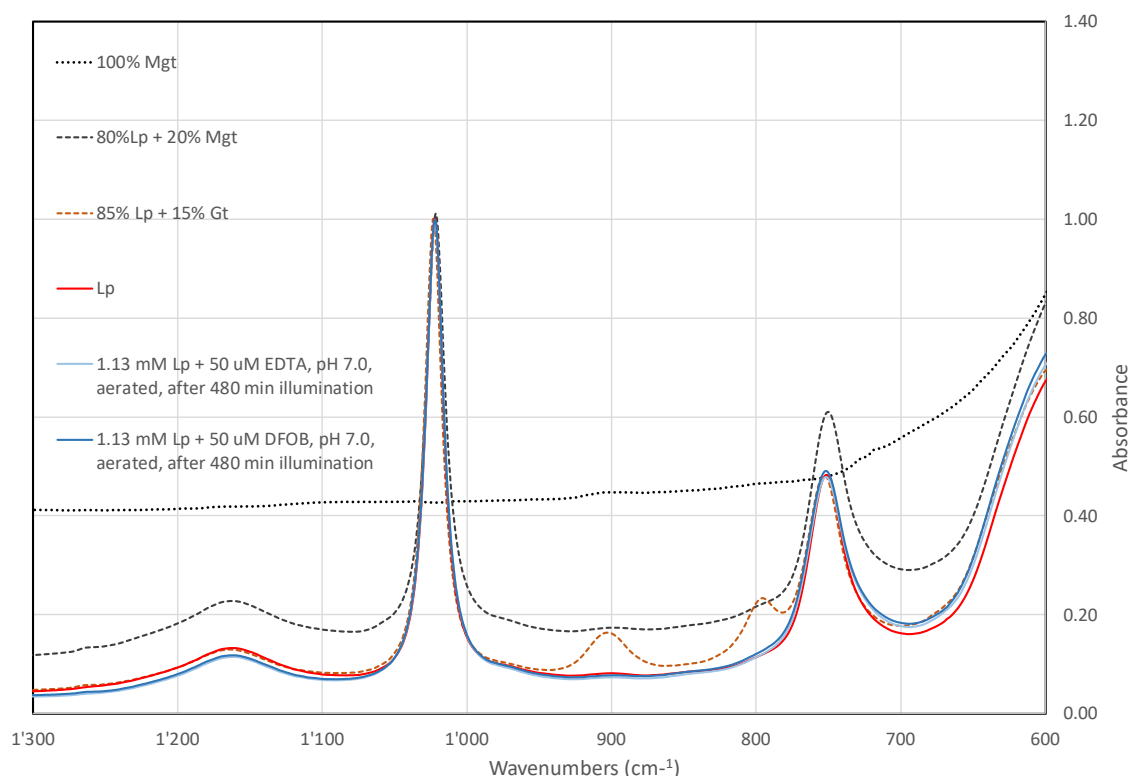


Figure S11. Infrared spectra of Lp before and after 480 min illumination with UV light in aerated suspensions of 1125 μM Lp and 50 μM EDTA or 50 μM DFOB at pH 7.0 (3 mM NaHCO_3 , 2% CO_2 in air). Samples (4 ml) were filtered through 4 mm diameter, 0.1 μm nylon filters. Collected solids in the filter were rinsed with 2 ml H_2O to remove most of the adsorbed ligands, and stored at -20°C until measurement of IR-spectra. Solids were re-suspended from the filter with 10-20 μl H_2O , and the suspensions were dried in a stream of N_2 on the 4 mm diameter diamond ATR-disk of the ATR-FTIR instrument (Biorad FTS 575C with 9-reflection diamond ATR unit from SensIR Technologies, Danbury, CT 06810-9931, USA). The spectra shown are the spectra of the dried solids. The spectra are compared to spectra of Lp before illumination, to Lp mixed with 15% Gt and to Lp with 20% magnetite (Mgt). For easier comparison, spectra were scaled to a common absorbance maximum of 1.0 for Lp at 1121 cm^{-1} . The detection of Mgt was not possible by characteristic bands, but by the broad absorbance of Mgt in this spectral range, as shown with by the spectrum of pure Mgt (100% Mgt). Based on the signals observed with the mixtures of Lp with Gt and Mgt, we estimate detections limits of $<3\%$ for Gt and Mgt in Lp. We thus detected no, or less than 3% Gt or Mgt after 480 min illumination at pH 7.0. The magnetite used was from MKnano, Fe_3O_4 , 99% pure, APS: 25 nm (M K Impex Corp. Mississauga, ON L5N 6X, Canada, <https://www.mknano.com/Nanoparticles/Single-Element-Oxides>).

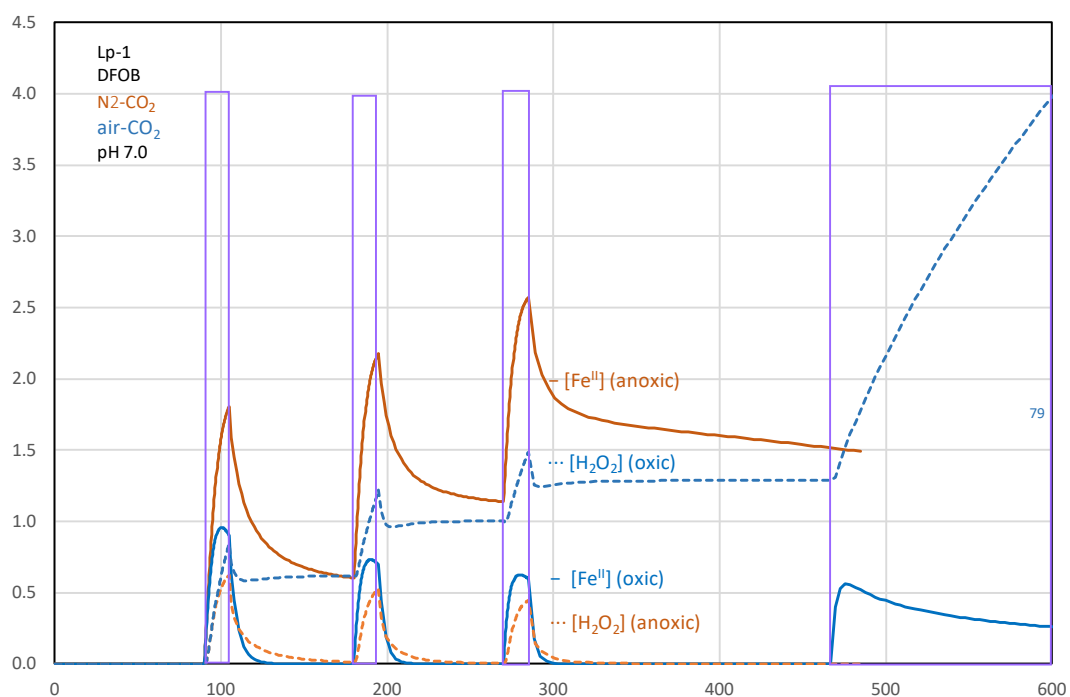


Figure S12. Calculated concentrations of Fe(II) (sum of dissolved and adsorbed Fe(II) species) and of dissolved H_2O_2 (μM) as a function of time (min) during the intermittent illumination (indicated with purple boxes) of Lp with DFOB. The corresponding concentrations of Fe_{diss} are shown in Fig. 3 in the main manuscript.

References

- Biswakarma, J., Kang, K., Borowski, S.C., Schenkeveld, W.D.C., Kraemer, S.M., Hering, J.G., Hug, S.J., 2019. Fe(II)-Catalyzed Ligand-Controlled Dissolution of Iron(hydr)oxides. *Environmental Science & Technology* 53, 88-97.
- Biswakarma, J., Kang, K., Schenkeveld, W.D.C., Kraemer, S.M., Hering, J.G., Hug, S.J., 2020. Linking Isotope-Exchange with Fe(II)-Catalyzed Dissolution of Iron (hydr)oxides in the Presence of Bacterial Siderophore Deferoxamine-B *Environmental Science & Technology* 54, 768-777.
- Braun, W., Herron, J.T., Kahaner, D.K., 1988. Acuchem: A computer program for modeling complex chemical reaction systems. *Int J Chem Kinet* 20, 51-62.
- Jones, A.M., Griffin, P.J., Collins, R.N., Waite, T.D., 2014. Ferrous iron oxidation under acidic conditions - The effect of ferric oxide surfaces. *Geochimica et Cosmochimica Acta* 145, 1-12.
- Kang, K., Schenkeveld, W.D.C., Biswakarma, J., Borowski, S.C., Hug, S.J., Hering, J.G., Kraemer, S.M., 2019. Low Fe(II) Concentrations Catalyze the Dissolution of Various Fe(III) (hydr)oxide Minerals in the Presence of Diverse Ligands and over a Broad pH Range. *Environmental Science & Technology* 53, 98-107.